Acetic acid gas sensors based on Ni^{2+} doped ZnO nanorods prepared by using the solvothermal method*

Cheng Zhiming(程志明)[1], Zhou Sumei(周素梅)[2], Chen Tongyun(陈同云)[2], Dong Yongping(董永平)[2], Zhang Wangbing(张王兵)[2], and Chu Xiangfeng(储向峰)[2,†]

[1]Department of Chemistry, School of Science, Beijing Jiaotong University, Beijing 100044, China
[2]School of Chemistry and Chemical Engineering, Anhui University of Technology, Maanshan 243002, China

Abstract: Ni^{2+}-doped ZnO nanorods with different doping concentrations are prepared via the solvothermal method. The doped ZnO nanorods are characterized by X-ray diffraction (XRD) and scanning electron microscopy (SEM), respectively. The amount of Ni^{2+} ions that enter the lattice of ZnO increases with increasing the Ni^{2+}/Zn^{2+} molar ratio when the molar ratio of Ni^{2+}/Zn^{2+} in the starting solution is lower than 3% and does not change obviously if the mole ratio of Ni^{2+}/Zn^{2+} in the starting solution is in the range of 3–10 mol%. The effect of Ni^{2+} doping on the gas-sensing properties is investigated. The results reveal that the amount of Ni^{2+} has a great influence on the response (R_a/R_g) and the gas-sensing selectivity. The sensor based on 1 mol % Ni^{2+} doped ZnO nanorods (120 ℃, 10 h) exhibits a high response to acetic acid vapor, in particular, the responses to 0.001 ppm and 0.01 ppm acetic acid vapor reach 1.6 and 2, respectively. The response time and the recovery time for 0.001 ppm acetic acid are only 4 s and 27 s, respectively.

Key words: ZnO; nanorods; gas sensor; acetic acid
DOI: 10.1088/1674-4926/33/11/112003 **EEACC:** 2520

1. Introduction

The gas sensing properties of one-dimensional nanomaterials have attracted extensive attention because they possess large surface area, thermal and mechanical stability are compatible with other nanodevices[1−4]. Doping is a good method to improve the physical properties of 1D nanomaterials[5−8]. The gas-sensitivity and selectivity of nanomaterials could also be improved by using the doping method. Kumar *et al.*[9] prepared Cu^{2+} doped SnO_2 nanowires through the thermal evaporation method and investigated the gas-sensing properties of a sensor based on Cu^{2+} doped SnO_2 nanowires, they found that Cu^{2+} entered the SnO_2 nanowire lattice and increased the sensitivity to H_2S for the film-type sensors based on SnO_2 nanowires. Hwang *et al.*[10] fabricated a CuO-functionalized SnO_2 nanowire sensor, Cu^{2+} did not enter the SnO_2 nanowire lattice and CuO distributed on the SnO_2 nano-wire surface uniformly, they found that the CuO coating increased the gas response to H_2S and the cross gas responses to NO_2, C_2H_5OH, and C_3H_8 were negligible. Cao *et al.*[11] prepared Nd-doped ZnO nanorods by low-temperature solid-state reaction, the results demonstrated that the sensor based on 2 at% Nd-doped ZnO nanorods presented much higher sensitivity, better selectivity, and a shorter response-recovery time to ethanol vapor than the pure ZnO nanorod sensor. Fan *et al.*[12] prepared Sm_2O_3-doped SnO_2 nanopowders with chemical deposition and revealed that the addition of Sm_2O_3 improves the C_2H_2 sensing properties of the SnO_2 gas sensor. Sun *et al.*[13] demonstrated that the addition of WO_3 can enhance the sensitivity of macro-porous silicon (MPS) to NO_2 and the long-term stability of a WO_3/MPS gas sensor is better than that of an MPS gas sensor

The main constituent of heroin is diacetylmorphine hydrochloride, diacetylmorphine hydrochloride will hydrolyze and an acetic acid vapor will be given off when diacetylmorphine hydrochloride comes into contact with water vapor in air; hence, heroin can be detected by means of detecting acetic acid vapor[14]. It is reported that the detection limits of acetic acid gas sensors are 2.35×10^{-4} g/ L (90 ppm)[14] and 10×10^{-6} (10 ppm)[15]. There are imperative needs for acetic acid gas sensors with a low detection limit because the concentration of acetic acid given off by the heroin hydrolysis reaction is very low.

In this paper, we prepared Ni^{2+} doped ZnO nanorods via the solvothermal method and investigated the effect of the Ni^{2+} doping on the gas response and selectivity. It was found that Ni^{2+} doping increased the response and selectivity to acetic acid vapor, especially, the 1 mol% Ni^{2+} doped ZnO nanorod sensor showed the best performance.

2. Experiment

The preparation method of 1D Ni^{2+} doped ZnO nanorods is similar to those reported in Refs. [5, 16]. A series of Ni^{2+} doped ZnO nanorod materials with different percentages of nickel ion were prepared using the same procedures. In a typical synthesis, 0.0005 mol $Zn(NO_3)_2{\cdot}6H_2O$ and different molar ratios of $Ni(NO_3)_2{\cdot}6H_2O$ were added into 10 mL C_2H_5OH,

* Project supported by the National Natural Science Foundation of China (No. 61271156), the Innovation Team Project of AHUT (No. TD201204), and the Research Project for University Personnel Returning from Overseas Sponsored by the Ministry of Education of China.
† Corresponding author. Email: xfchu99@ahut.edu.cn
Received 9 April 2012, revised manuscript received 6 June 2012

and the solution was stirred for 30 min. 0.50 M NaOH ethanol solution [the molar ratio of $(n_{Ni2+} + n_{Zn2+})/n_{NaOH}$ was 1/2] was dropped into the above solution slowly, the mixture was then transferred into a teflon-lined autoclave (20 mL) and kept at a certain temperature for different times in an oven. The product was collected and washed with distilled water and ethanol to remove by-products, and finally dried at 80 ℃ for 10 h. The phase composition of the samples was characterized using X-ray diffraction (XRD, D8 Advance, 40 kV and 40 mA). The morphology of the material particles was investigated by scanning electron microscopy (SEM, X-650).

A paste was prepared from a mixture of ZnO with a PVA (polyvinyl alcohol) solution, the paste was coated with a small brush onto an Al_2O_3 tube on which two gold leads had been installed at each end. The Al_2O_3 tube was about 8 mm in length, 2 mm in external diameter and 1.6 mm in internal diameter. The Al_2O_3 tube was heated in air at 500 ℃ for 0.5 h to remove PVA after it was dried at 80 ℃. A heater of Ni-Cr wire was inserted into the Al_2O_3 tube to supply the operating temperature that could be controlled in a range of 80–500 ℃.

The electrical resistance of the sensor was measured in air and in the mixture of detected gas and air. The relative humidity in air was about 55%. The response is defined as the ratio of the electrical resistance of the sensor in air (R_a) to that in the mixture of detected gas and air (R_g) when the resistance of the sensor reaches a stable value. The preparation method for mixture of the detected gas and air was described in our previous work[17]. When measuring the electrical resistance of a sensor in air, the sensor was placed in a closed glass bottle filled with pure air and the surface temperature of the sensor was adjusted to operating temperature by changing the voltage and the current of the heater wire. The sensor was placed in the air bottle for at least 5 min after the electrical resistance of the sensor was stable, then the sensor was taken out from the air bottle and placed in a closed bottle filled with the mixture of detected gas and air. If the resistance of the sensor could not recover from the previous exposure, we adjusted the operating temperature to 350–400 ℃ and maintained the operating temperature for about 10 min to let the detected gas desorb outside the air bottle. The resistance change of the sensor was recorded by a computer.

3. Results and discussion

The typical XRD patterns of the samples prepared under 100 ℃ for 10 h with various levels of nickel dopant are presented in Fig. 1. The main diffraction peaks in Fig. 1(a) can be indexed to hexagonal wurtzite structure ZnO (JCPDS card no.36-1451), there is no peak of impurities in all the samples. It should be noted that NiO or $Ni(OH)_2$ are not observed in all of the samples even though the molar ratio of Ni^{2+} to Zn^{2+} in the starting solution reaches 10%. ZnO is the unique phase in the all samples, which reveals that Ni^{2+} ions enter the lattice of ZnO and occupy the sites of Zn^{2+}. But the crystalline sizes decrease slightly when the concentration of Ni^{2+} increases [see the peaks (100) and (101) in Fig. 1(a)]. As shown in Fig. 1(b), the positions of (002) peaks of pure ZnO, 1 mol% Ni^{2+} doped ZnO and 3 mol% Ni^{2+} doped ZnO are 34.50°, 34.54° and 34.58°, respectively. The position shift of the peak (002) is very small. The shift of the (002) peak to a higher angle is caused

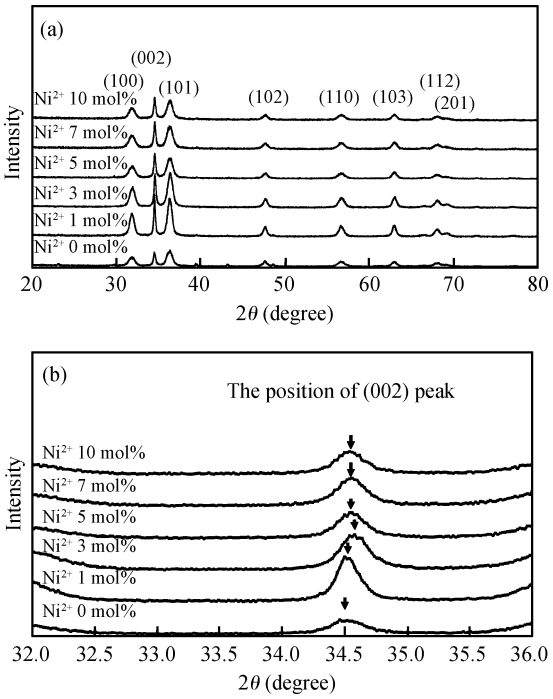

Fig. 1. (a) The typical XRD patterns of samples prepared under 100 ℃, 10 h with various levels of nickel dopant. (b) The (002) peak positions of all samples in enlarged XRD patterns.

by the difference between Ni^{2+} radius (0.69 Å) and Zn^{2+} radius (0.74 Å), the results are similar to those reported by Zhang *et al.*[5]. The positions of the (002) peaks of 5 mol% Ni^{2+} doped ZnO, 7 mol% Ni^{2+} doped ZnO and 10 mol% Ni^{2+} doped ZnO are close to that of 3 mol% Ni^{2+} doped ZnO, indicating that excessive Ni^{2+} ions do not enter the lattice of ZnO. Our preparation method is similar to that reported by Iqbal *et al.*[8], the molar ratio of Ni^{2+} to Zn^{2+} was 6/100 in their starting material, they found that only 3 mol% Ni^{2+} entered the lattice, indicating that not all Ni^{2+} ions in the starting solution entered the ZnO lattice. Wu *et al.*[18] prepared Ni^{2+} doped ZnO rod arrays from aqueous solution, and the amount of Ni^{2+} incorporated into the ZnO matrix was much less than the actual amount of Ni^{2+} provided in the precursor during synthesis, NiO peaks could not be found in the XRD patterns even when the molar ratio of Ni^{2+} to Zn^{2+} in the starting material reached 0.4, they attributed this phenomenon to the formation of a mass of fine NiO clusters in the reactive solution, which were discarded in the purification steps. We think that a small amount of NiO probably exist in our samples and could not induce detectable peaks in XRD patterns because the NiO phase cannot be detected by XRD if the NiO/ZnO weight ratio is lower than about 2%.

Figure 2 shows the SEM images of the Ni^{2+} doped ZnO samples prepared under different conditions. The morphology of the Ni^{2+} doped ZnO samples prepared under different conditions is that of nanorods, the sizes of the nanorods are slightly affected by the solvothermal conditions. As shown in Figs. 2(a), 2(c), and 2(e), the sizes of 3 mol% Ni^{2+} doped ZnO nanorods in the samples prepared under different temperatures increase with the solvothermal temperature increasing. It can be seen from Figs. 2(b), 2(c), and 2(d) that the sizes of

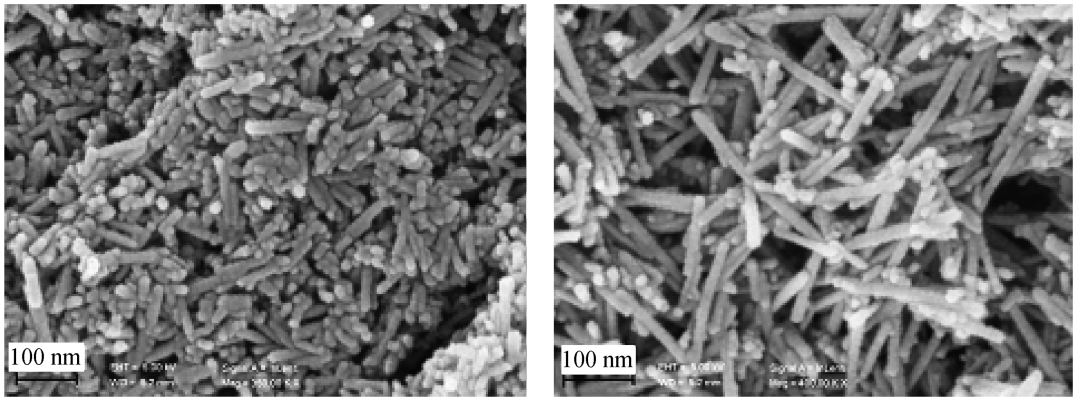

(a) 80 ℃, 10 h, 3% Ni^{2+} doped ZnO (b) 100 ℃, 5 h, 5% Ni^{2+} doped ZnO

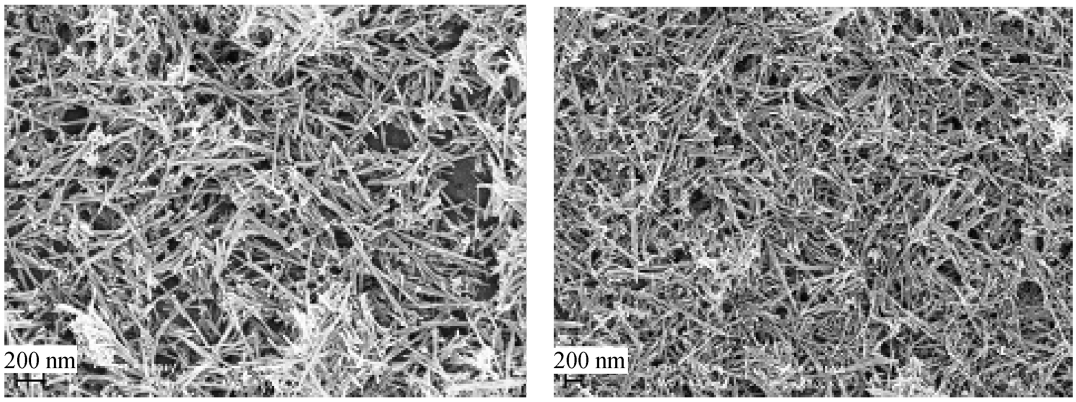

(c) 100 ℃, 10 h, 3% Ni^{2+} doped ZnO (d) 100 ℃, 15 h, 3% Ni^{2+} doped ZnO

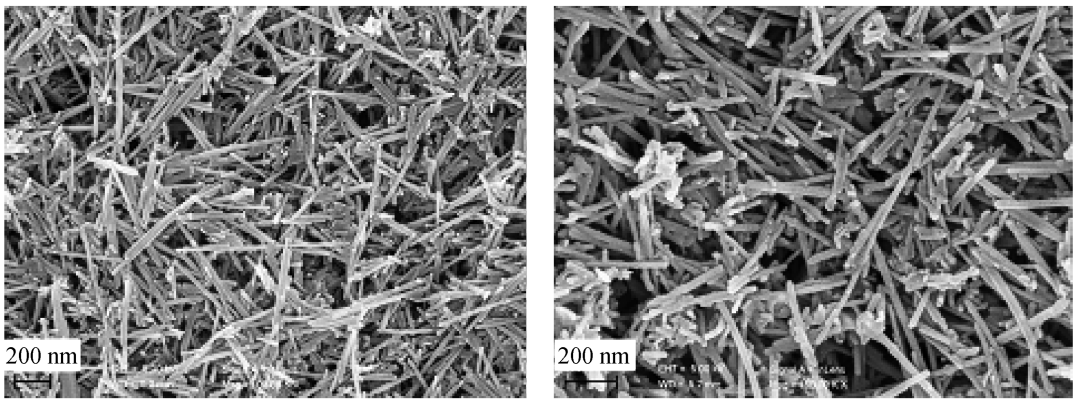

(e) 120 ℃, 10 h, 3% Ni^{2+} doped ZnO (f) 120 ℃, 10 h, 1% Ni^{2+} doped ZnO

Fig. 2. SEM images of the Ni^{2+} doped ZnO samples prepared under different conditions.

3 mol% Ni^{2+} doped ZnO nanorods in the samples also increase with the hydrothermal duration increasing. The diameters and the lengths of the rods in the sample prepared under 120 ℃, 10 h are 20–60 nm and 100–800 nm, respectively. The sizes of 1 mol% Ni^{2+} doped ZnO nanorods in the sample prepared at 120 ℃ for 10 h shown in Fig. 2(f) are almost same as those 3 mol% Ni^{2+} doped ZnO nanorods in the sample prepared under the same conditions, indicating that doping concentration exerts less influence on the sizes of the nanorods.

Figure 3 shows the electrical resistances of a pure ZnO sensor and Ni^{2+} doped sensors in air at different operating temperatures (preparation conditions of pure ZnO and Ni^{2+} doped ZnO: 120 ℃, 10 h). The resistances of all sensors decrease with the operating temperature increasing because the resistance of the semiconductor material decreases with increasing the temperature. It is observed that the resistances of all Ni^{2+} doped ZnO sensors are higher than ZnO sensor and the resistances of doped ZnO sensors increase with increasing the Ni^{2+} doping concentration, indicating that all Ni^{2+} ions do not enter the lattice of ZnO and some Ni^{2+} ions exist in the form of NiO nanoparticles that distribute on the surface of the Ni^{2+} doped ZnO nanorods. If there is no NiO in the samples besides Ni^{2+} at Zn^{2+} sites in the ZnO lattice, the resistances of the Ni^{2+} doped ZnO sensors will not increase with increasing the Ni^{2+} doping concentration because the valances of Ni^{2+} and Zn^{2+} are the same. The preparation method in our experiments is

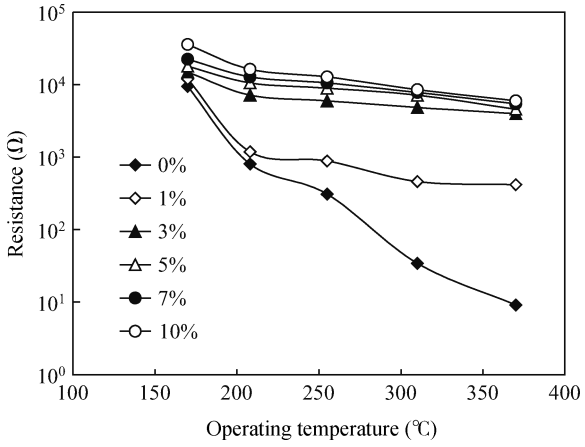

Fig. 3. The electrical resistances of the pure ZnO sensor and Ni^{2+} doped ZnO sensors in air at different operating temperatures (preparation conditions of pure ZnO and Ni^{2+} doped ZnO: 120 ℃, 10 h).

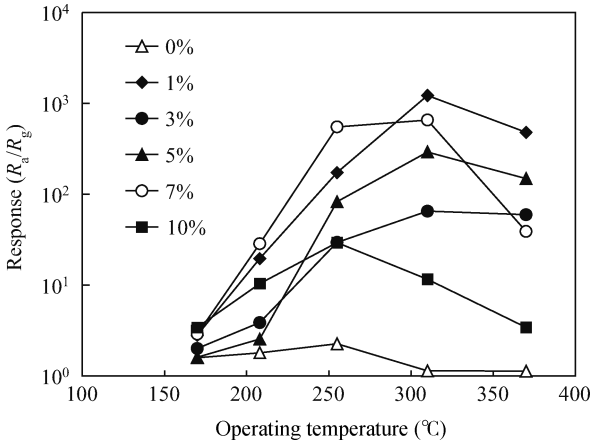

Fig. 4. The effect of the Ni^{2+} doping on the responses to 1000 ppm acetic acid gas of sensors based on doped ZnO nanorods (120 ℃, 10 h).

similar to that used in Ref. [18], they also found that only a few Ni^{2+} were doped into the ZnO lattice, this phenomenon was consistent with the conclusion from UV-visible absorption spectra. It is believed that some heterogeneous inter-grain boundaries of NiO (p-type)-ZnO (n-type) can form in the Ni^{2+} doped ZnO nanorod materials. This results in the formation of barrier height among the grains and hence increases the resistances of the Ni^{2+} doped ZnO nanorod sensors. Wang *et al.*[19] prepared Cr_2O_3-sensitized ZnO nanofibers and investigated their ethanol-sensing properties, they also found these phenomena: firstly, there is no Cr_2O_3 phase in ZnO nanofiber samples even when the Cr_2O_3/ZnO weight ratio was 8.5%; secondly, the resistances of Cr_2O_3 doped ZnO nanofiber sensors increased with Cr_2O_3 content increasing in the starting solution; thirdly, the sensitivity to ethanol of Cr_2O_3 doped ZnO nanofiber sensors increased with Cr_2O_3 content increasing when the Cr_2O_3/ZnO weight ratio is lower than 4.5% and decreased when the Cr_2O_3/ZnO weight ratio is higher than 4.5%. They ascribed these phenomena to the existence of Cr_2O_3 in the materials and the heterogeneous inter-grain boundaries of ZnO–Cr_2O_3 (p–n junction).

Figure 4 depicts the response values of the sensors based on pure ZnO and Ni^{2+} doped ZnO (120 ℃, 10 h) to 1000 ppm acetic acid gas at different operating temperatures. It is found that the responses of the sensors vary with the change of the amount of Ni^{2+} dopant as well as the operating temperature variation. The responses of the sensor based on pure ZnO at different operating temperatures are very low and the maximum response is only 2.6. The sensors based on Ni^{2+} doped ZnO with different amounts of dopant exhibit higher responses than the sensor based on pure ZnO, but it is difficult to obtain the relationship between the response and the amount of dopant. In order to examine the reproducibility, the maximum responses of the sensors fabricated with two batch of Ni^{2+} doped ZnO (same Ni^{2+} content in the starting materials) show same change tendency and the response deviation of two sensors fabricated with two batches of materials prepared under same conditions do not exceed 15%. The maximum response of the sensor based on 1 mol% Ni^{2+} doped ZnO nanorods is higher than those of the sensors based on 3–10 mol% Ni^{2+} doped ZnO nanorods. The maximum response of the sensor based on 1 mol% Ni^{2+} doped ZnO nanorods reaches 1219 when operating at 310 ℃. The gas sensing mechanisms of the pure ZnO sensors and doped ZnO sensors have been explained by authors[19−21]. The surface of the ZnO nanorods adsorbs oxygen molecules, and then the adsorbed oxygen molecules capture electrons from the conduction band of the ZnO nanorods and exist in the form of O_2^-, O_2^{2-} and O^{2-} at different operating temperatures. When the ZnO nanorods are exposed to reducing gas, the reducing gas will adsorb on the surface of the sensing material and react with the adsorbed oxygen, releasing the trapped electrons back to the conduction band, and then the resistance of the sensor based on ZnO nanorods decreases. The response improvement was attributed to the presence of p–n heterogeneous inter-grain boundaries in the Cr^{3+} doped ZnO nano-fiber sensor[19], the Ni^{2+} doped ZnO tetrapod sensor[22], and the Ni^{2+} doped SnO_2 sensor[23]. According to the above literatures[19, 22], the response improvement of Ni^{2+} doped nanorod sensors may be explained as follows. The total amount of p–n heterojunction and ZnO barriers is certain in the Ni^{2+} doped ZnO nanorod film and the change of p–n heterojunction barrier resulted from the action of chemical oxygen absorption is much less than that of the ZnO barrier. If the quantity of p–n heterojunctions is too large, the quantity of ZnO barriers is small; the change of the sensor resistance resulting from the reaction between the detected gas and absorption oxygen on ZnO surface is small, which leads to a low response. The response cannot be improved adequately if the concentration of p–n heterojunctions is too low. When the ratio of the p–n junctions to the Schottky barriers on thick film surface is optimized, the maximum response can be obtained. The ratio of the p–n junctions to the Schottky barriers is relative to NiO concentration and NiO distribution in Ni^{2+} doped ZnO nanorod materials. The ratio of the p–n junctions to the Schottky barriers on a thick film surface attains an optimum value in 1 mol% Ni^{2+} doped ZnO nanorod material and the sensor exhibits the highest response. A similar phenomenon was also reported by Liu *et al.*[24] for $La_{1-x}Mg_xFeO_3$ materials, the optimal response of the $La_{1-x}Mg_xFeO_3$ sensor to 1000 ppm methane increases up to a maximum value of 8.48 at $x = 0.1$

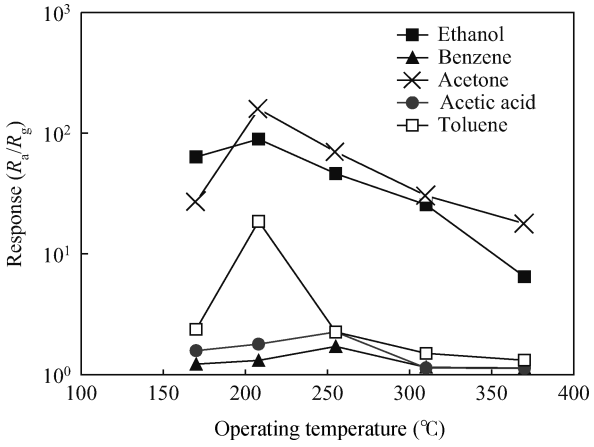

Fig. 5. The responses of the sensors based on pure ZnO nanorods (120 ℃, 10 h) to 5 kinds of gases.

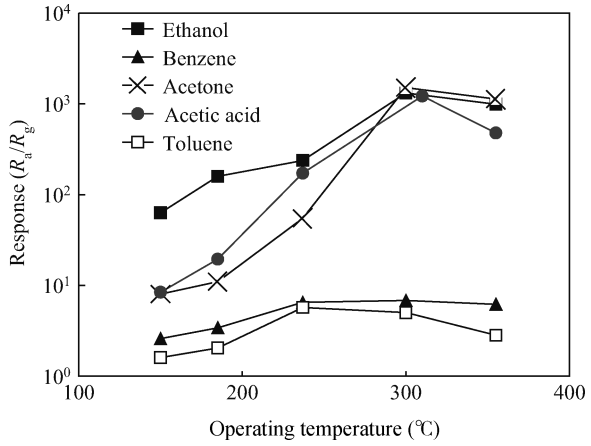

Fig. 6. The responses of the sensors based on 1 mol% Ni^{2+} doped ZnO nanorods (120 ℃, 10 h) to 5 kinds of gases.

and falls off dramatically; the optimal response increases again at $x = 0.5$ and decreases at $x = 0.7$. They also attributed this phenomenon to the proper proportion of p–n hetero-junctions in the materials.

The responses of the sensors based on pure ZnO and 1 mol% Ni^{2+} doped ZnO nanorods (120 ℃, 10 h) to 5 kinds of gases are shown in Figs. 5 and 6. The responses to 5 kinds of gases are all enhanced to some extent by doping 1 mol% Ni^{2+}, but the responses to 1000 ppm acetic acid gas are improved obviously comparing with the responses to other 4 kinds of gases; the maximum response to 1000 ppm acetic acid gas of the pure ZnO sensor is only 2.3, while the maximum response to 1000 ppm acetic acid gas of the 1 mol% Ni^{2+} doped ZnO sensor reaches 1219. It is easy to understand the low responses to benzene and toluene of the sensors based on pure ZnO and 1 mol% Ni^{2+} doped ZnO nanorods because the benzene ring is stable and cannot be oxidized easily. At present, the reason why doping can change the responses of the materials to different gases in different manners is very complicated and is not explained clearly in many literatures. Zheng *et al.*[25] attributed the good selectivity to HCHO gas of the NiO-doped SnO_2 sensor to the enhanced reaction between HCHO and adsorbed oxygen at an optimum operating temperature. As far as

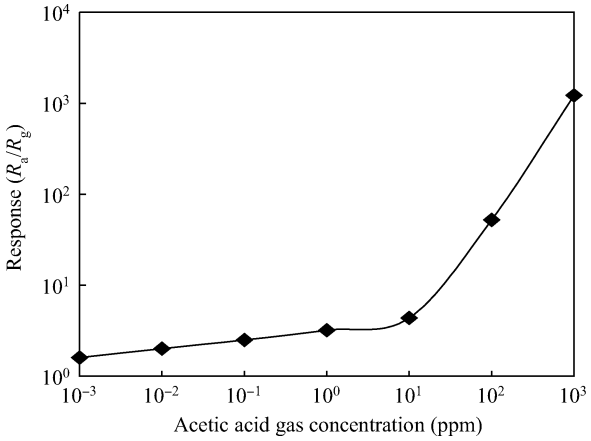

Fig. 7. The relationship between the responses of the sensor based on 1 mol% Ni^{2+} doped ZnO nanorods (120 ℃, 10 h) and the acetic acid gas concentration when operating at 310 ℃.

NiO-doped ZnO nanorod materials are concerned, the selectivity change maybe result from the variation of the adsorption ability of different gases. The sensor based on 1 mol% Ni^{2+} doped ZnO nanorods also exhibits high responses to ethanol and acetone. Hence, the sensor can only be applied in the atmosphere in which there is no ethanol and acetone.

Figure 7 depicts the relationship between the responses of the sensor based on 1 mol% Ni^{2+} doped ZnO nanorods (120 ℃, 10 h) and the acetic acid gas concentration when operating at 310 ℃. The responses increase with increasing the acetic acid gas concentration slowly when the concentration is lower than 10 ppm, and increase quickly if the concentration exceeds 10 ppm. The curve of response versus gas concentration (R–c) can be divided into two linear sections in the concentration ranges of 0.001–10 ppm and 10–1000 ppm, respectively. The response to 0.001 ppm acetic acid gas concentration reaches 1.6. The detection limit is higher than those reported by previous literatures[14, 15]. In general, the shape of the curve of R–c is S-shaped in a large range of gas concentration. the response reaches saturation when the gas concentration is too high[19]; the relation between the response and gas concentration follows the formula $R = Ac^{\beta}$ in a concentration range depended by sensing material, where c is gas concentration, A and β are constants for certain materials[26, 27]; the response does not increase or increases very slowly with the gas concentration increasing when the gas concentration is low[27], the reason is probably that there are two different adsorption mechanisms for the detected gas.

Response-recovery characteristics are very important parameters of the gas sensor. In general, the response time and recovery time are defined as the times for a sensor to reach 90% of the final signal. The response transients of the sensor based on 1 mol% Ni^{2+} doped ZnO nanorods (120 ℃, 10 h) to 0.001, 0.01 and 100 ppm acetic acid gas at 310 ℃ are shown in Fig. 8. The response time and recovery time for 0.001 ppm acetic acid gas are 4 s and 27 s; the response time and recovery time for 100 ppm acetic acid gas are 14 s and 23 s. The response of the sensor based on pure ZnO nanorods to 100 ppm acetic acid is only 1.2 at 310 ℃; the response time and recovery time for 100 ppm acetic acid gas are 16 s and 26 s. Comparing the

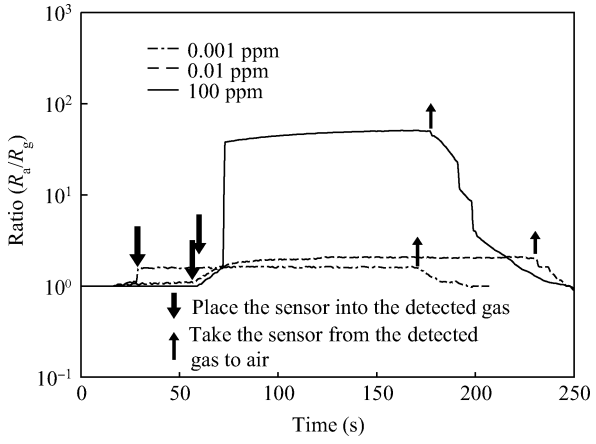

Fig. 8. The response transients of the sensor based on 1 mol% Ni^{2+} doped ZnO nanorods (120 ℃, 10 h) to 0.001, 0.01 and 100 ppm acetic acid gas at 310 ℃.

response time and the recovery time of the Ni^{2+} doped ZnO sensor for 100 ppm with those of the pure ZnO nanorod sensor, Ni^{2+} doping has less influence over the response time and the recovery time. In order to examine the reproducibility, three sensors is fabricated using 1 mol% Ni^{2+} doped ZnO nanorod material (120 ℃, 10 h) at a time, although the maximum resistance error of the three sensors at the same operating temperature reaches 18% because the thickness of the films of three sensors is not the same, the response deviations of the three sensors at the same operating temperature do not exceed 6%.

4. Conclusion

In summary, the responses of sensors based on ZnO nanorods are enhanced by doping Ni^{2+}. The sensor based on 1 mol% Ni^{2+} doped ZnO nanorods exhibits a high response to acetic acid vapor. The responses to 0.001 ppm and 0.01 ppm acetic acid vapor reached 1.6 and 2, respectively. The response time and the recovery time for 0.001 ppm acetic acid are 4 s and 27 s, respectively. The sensor is a potential candidate for detecting heroin via measuring the acetic acid vapor.

References

[1] Lupana O, Chaic G, Lee C. Novel hydrogen gas sensor based on single ZnO nanorod. Microelectron Eng, 2008, 85(11): 2220

[2] Huang Jiarui, Wang Junhai, Zhukova A A, et al. High-sensitivity humidity sensor based on a single Sb-doped SnO_2 Whisker. Sensor Lett, 2009, 7(6): 1025

[3] Patil D R, Kale D D, Patil S R, et al. Novel method for synthesis of ZnO nanorods and its applications as highly selective chlorine sensors working at low temperature. Sensor Lett, 2009, 7(6): 1057

[4] Cao Yali, Jia Dianzeng, Huang Yudai, et al. Facile one-step solid-state chemical synthesis and gas-sensing property of ZnO nanorods. Sensor Lett, 2009, 7(2): 110

[5] Zhang Xiaoli, Qiao Ru, Qiu Ri, et al. Synthesis and magnetic properties of one-dimensional zinc nickel oxide solid solution. J Phys Chem A, 2007, 111 (20): 4195

[6] Bhisea A B, Latea D J, Walkeb P S, et al. Sb-doped SnO_2 wire: highly stable field emitter. J Cryst Growth, 2007, 307(1): 87

[7] Jia Tiekun, Wang Weimin, Long Fei, et al. Fabrication, characterization and photocatalytic activity of La-doped ZnO nanowires. Journal of Alloys and Compounds, 2009, 484(1/2): 410

[8] Iqbal J, Wang Baiqi, Liu Xiaofang, et al. Oxygen-vacancy-induced green emission and room-temperature ferromagnetism in Ni-doped ZnO nanorods. New J Phys, 2009, 11: 063009

[9] Kumara V, Senb S, Mutheb K P, et al. Copper doped SnO_2 nanowires as highly sensitive H_2S gas sensor. Sensors and Actuators B, 2009, 138(2): 587

[10] Hwanga I S, Choia J K, Kima S J, et al. Enhanced H_2S sensing characteristics of SnO_2 nanowires functionalized with CuO. Sensors and Actuators B, 2009, 142(1): 105

[11] Cao Yali, Pan Weiyu, Zong Ying, et al. Preparation and gas-sensing properties of pure and Nd-doped ZnO nanorods by low-heating solid-state chemical reaction. Sensors and Actuators B, 2009, 138(2): 480

[12] Fan H T, Zhang T, Qi Q, et al. Preparation and C_2H_2 sensing characteristics of Sm_2O_3-doped SnO_2 gas sensors. Journal of Semiconductors, 2008, 29(2): 319

[13] Sun P, Hu M, Ling M D, et al. Nano-WO_3 film modified macroporous silicon (MPS) gas sensor. Journal of Semiconductors, 2008, 29(2): 319

[14] Sun Y F, Wang L C, Huang X J, et al. Fast detecting method of heroine based on acetic acid gas sensor. Journal of Transducer Technology, 2004, 23(2): 8

[15] Jiao Z, Bian L, Liu J. The preparation and research on sensitive characteristics of heroine detection acetic acid sensor. Instrument Technique and Sensor, 2001, (5): 12

[16] Chu Dewei, Zeng Yuping, Jiang Dongliang. Synthesis and growth mechanism of Cr-doped ZnO single-crystalline nanowires. Solid State Commun, 2007, 143(6/7): 308

[17] Chu Xiangfeng, Chen Tongyun, Zhang Wangbing, et al. Investigation on formaldehyde gas sensor with ZnO thick film prepared through microwave heating method. Sensors and Actuators B, 2009, 142(1): 49

[18] Wu Dianwu, Yang Mei, Huang Zhongbing, et al. Preparation and properties of Ni-doped ZnO rod arrays from aqueous solution. Journal of Colloid and Interface Science, 2009, 330(2): 380

[19] Wang Wei, Li Zhenyu, Zheng Wei, et al. Cr_2O_3-sensitized ZnO electrospun nanofibers based ethanol detectors. Sensors and Actuators B, 2010, 143(2): 754

[20] Lin F C, Takao Y, Shimizu Y, et al. Hydrogensensing mechanism of zinc oxide varistor gas sensors. Sensors and Actuators B, 1995, 25(1–3): 843

[21] Yang Zunxian, Huang Yun, Chen Guonan, et al. Ethanol gas sensor based on Al-doped ZnO nanomaterial with many gas diffusing channels. Sensors and Actuators B, 2009, 140(2): 549

[22] Bai Z, Xie C, Hu M, et al. Formaldehyde sensor based on Ni-doped tetrapod-shaped ZnO nanopowder induced by external magnetic field. Physica E, 2008, 41(2): 235

[23] Jain K, Pant R P, Lakshmikumar S T. Effect of Ni doping on thick film SnO_2 gas sensor. Sensors and Actuators B, 2006, 113(2): 823

[24] Liu Xing, Cheng Bin, Hu Jifan, et al. Preparation, structure, resistance and methane-gas sensing properties of nominal $La_{1-x}Mg_xFeO_3$. Sensors and Actuators B, 2008, 133(1): 340

[25] Zheng Yangong, Wang Jing, Yao Pengjun. Formaldehyde sensing properties of electrospun NiO-doped SnO_2 nanofibers. Sensors and Actuators B, 2011, 156(2): 723

[26] Li L M, Li C C, Zhang J, et al. Bandgap narrowing and ethanol sensing properties of In-doped ZnO nanowires. Nanotechnology, 2007, 18: 225504

[27] Malyshev V V, Pislyakov A V. Investigation of gas-sensitivity of sensor structures to carbon monoxide in a wide range of temperature, concentration and humidity of gas medium. Sensors and Actuators B, 2007, 123(1): 71